AFRL-RY-WP-TP-2013-0030

LATEST PROGRESS IN HIGH POWER VECSELs (POSTPRINT)

Robert Bedford

Optoelectronic Technology Branch
Aerospace Components & Subsystems Division

Chris Hessenius, Jerome Moloney, and Mahmoud Fallahi

Univerity of Arizona

Nathan Terry

United States Air Force Academy

JANUARY 2013
Interim

AIR FORCE RESEARCH LABORATORY
SENSORS DIRECTORATE
WRIGHT-PATTERSON AIR FORCE BASE, OH 45433-7304
AIR FORCE MATERIEL COMMAND
UNITED STATES AIR FORCE

REPORT DOCUMENTATION PAGE

Form Approved
OMB No. 0704-0188

1. REPORT DATE *(DD-MM-YY)*	2. REPORT TYPE	3. DATES COVERED *(From - To)*
January 2013	Technical Paper	1 October 2006 – 11 January 2011

4. TITLE AND SUBTITLE
LATEST PROGRESS IN HIGH POWER VECSELs (POSTPRINT)

5a. CONTRACT NUMBER
In-house

5b. GRANT NUMBER

5c. PROGRAM ELEMENT NUMBER
62204F

6. AUTHOR(S)
Robert Bedford (AFRL/RYDH)
Chris Hessenius, Jerome Moloney, and Mahmoud Fallahi (University of Arizona)
Nathan Terry (United States Air Force Academy)

5d. PROJECT NUMBER
2002

5e. TASK NUMBER
IH

5f. WORK UNIT NUMBER
Y053

7. PERFORMING ORGANIZATION NAME(S) AND ADDRESS(ES)
Optoelectronic Technology Branch
Aerospace Components & Subsystems Division
Air Force Research Laboratory, Sensors Directorate
Wright-Patterson Air Force Base, OH 45433-7320
Air Force Materiel Command, United States Air Force

University of Arizona
United States Air Force Academy

8. PERFORMING ORGANIZATION REPORT NUMBER
AFRL-RY-WP-TP-2013-0030

9. SPONSORING/MONITORING AGENCY NAME(S) AND ADDRESS(ES)
Air Force Research Laboratory
Sensors Directorate
Wright-Patterson Air Force Base, OH 45433-7320
Air Force Materiel Command
United States Air Force

Air Force Office of Scientific Research AFOSR
875 North Randolph Street, Suite 325, Room 3112
Arlington, VA 22203-1768

10. SPONSORING/MONITORING AGENCY ACRONYM(S)
AFRL/RYDH

11. SPONSORING/MONITORING AGENCY REPORT NUMBER(S)
AFRL-RY-WP-TP-2013-0030

12. DISTRIBUTION/AVAILABILITY STATEMENT
Approved for public release; distribution unlimited.

13. SUPPLEMENTARY NOTES
Journal article published in Proc. SPIE 7945, 794508-1-9, 2011. ©2011 SPIE. The U.S. Government is joint author of the work and has the right to use, modify, reproduce, release, perform, display or disclose the work. PAO Case Number 88ABW-2010-6313, Clearance Date 1 December 2010. Report contains color.

14. ABSTRACT
Vertical external cavity surface emitting lasers (VECSELs) have captured the interest of high-brightness semiconductor researchers, primarily due to their simplicity in design, power scalability, and "open cavity architecture," wherein it is simple to integrate nonlinear elements into the cavity. Through direct emission and indirect (frequency-converted) means, wavelengths from the UV through to the mid-wave infrared regimes have been demonstrated, increasing the suitability of the VECSEL platform for multiple applications. This presentation outlines recent progress in VECSELs, measurements, novel cavities, and potential applications for these lasers.

15. SUBJECT TERMS
Semiconductor, lasers

16. SECURITY CLASSIFICATION OF:			17. LIMITATION OF ABSTRACT:	18. NUMBER OF PAGES	19a. NAME OF RESPONSIBLE PERSON (Monitor)
a. REPORT	b. ABSTRACT	c. THIS PAGE			Robert Bedford
Unclassified	Unclassified	Unclassified	SAR	12	19b. TELEPHONE NUMBER *(Include Area Code)* N/A

Invited Paper

Latest Progress in High Power VECSELs

Robert G. Bedford[a], Nathan Terry[b], Chris Hessenius[c], Mahmoud Fallahi[c], and Jerome Moloney[c]

[a]Air Force Research Laboratory, Wright-Patterson Air Force Base, Ohio
[b]Department of Physics, United States Air Force Academy, Colorado
[c]College of Optical Sciences, University of Arizona, Tucson, Arizona

ABSTRACT

Vertical external cavity surface emitting lasers (VECSELs) have captured the interest of high-brightness semiconductor researchers, primarily due to their simplicity in design, power scalability, and "open cavity architecture," wherein it is simple to integrate nonlinear elements into the cavity. Through direct emission and indirect (frequency-converted) means, wavelengths from the UV through to the mid-wave infrared regimes have been demonstrated, increasing the suitability of the VECSEL platform for multiple applications. This presentation outlines recent progress in VECSELs, measurements, novel cavities, and potential applications for these lasers.

1. INTRODUCTION

Throughout the last two decades, high-brightness semiconductor lasers have been an important interest, pursuit, and challenge for researchers. In many cases, the motivation for this research is to replace the lower efficiency, larger, complicated solid-state laser systems. In contrast, semiconductor material often exhibits, allows for more varied wavelengths, are more efficient, and can be tailored to an application.

In this manuscript we lay out some advantages to VECSELs as compared to many in-plane semiconductor lasers. We review common fabrication and packaging techniques in Section 2. In Section 3, we discuss both small-signal and large-signal dynamics governing VECSELs, including the fact that they lay on an interesting regime between class-A and class-B lasers. We then make some comments on some novel VECSEL cavity possibilities in Section 4. We provide some concluding remarks in Section 5.

1.1 In-plane lasers

In plane semiconductor lasers, confine in the transverse (growth) direction by index guiding, and in the lateral direction by either index guiding like that provided in ridge lasers, or by gain guiding, which is most often associated with broad-area multi-mode devices. It should be noted that because gain volumes are often significantly smaller than solid-state alternatives, semiconductor lasers don't produce more power than solid-state alternatives. Nevertheless, power should scale with gain volume, therefore increasing the laser length and gain/mode width allows for increased power. Gain saturation limits the practical gain lengths achievable, while the desire to remain operating in a single spatial mode limits the lateral size of the device. Semiconductor material tends to have a strong amplitude phase, which can be described by the relation between the real part imaginary part of the refractive index, and "filaments" can form which break up the spatial coherence of the laser.[1]

As the mode is typically confined to a few microns in the transverse direction, the power density at the facet is large, and can cause catastrophic damage.[2] Moreover, the mode, especially for higher powers, can be very elliptical and astigmatic, often which is undesirable for the application. Some manifestations of edge-emitting lasers, such as the slab-coupled optical waveguide laser (SCOWL) have addressed this issue by creating a waveguide which reaches farther into the substrate, and has a lower gain-overlap.[3] The large mode size of the SCOWL means they are able to obtain higher brightness operation, although the single-mode size is still limited to nominally 30×10^{-8} cm^2, and therefore practical single-emitter powers remain at around 2 W or less.

Further author information (RGB): e-mail: robert.bedford@wpafb.af.mil

Quantum Sensing and Nanophotonic Devices VIII, edited by Manijeh Razeghi, Rengarajan Sudharsanan, Gail J. Brown, Proc. of SPIE Vol. 7945, 794508 · © 2011 SPIE · CCC code: 0277-786X/11/$18 · doi: 10.1117/12.873871

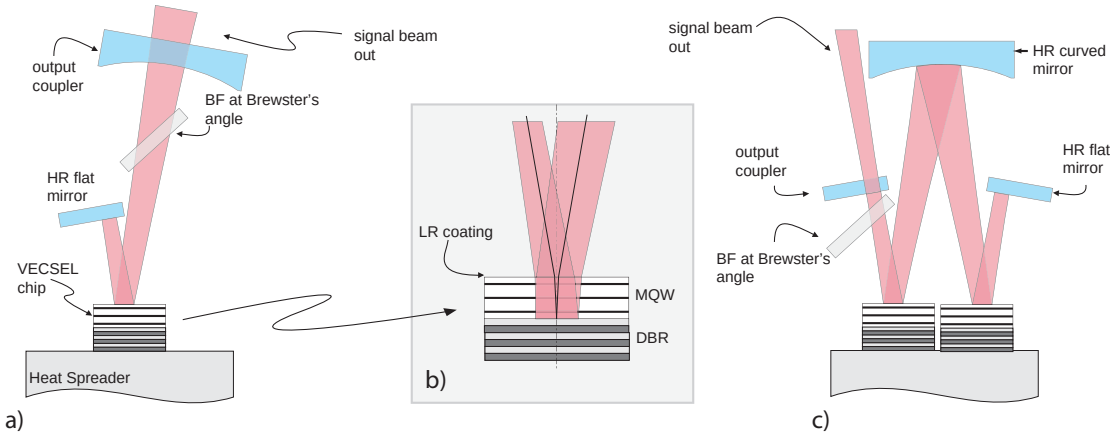

Figure 1. a)Schematic of a "v-cavity" VECSEL, where the gain chip is at a fold of the cavity. b) zoomed-in components of the VECSEL chip. c) an example of a multi-chip cavity for power scaling.

1.2 Vertical cavity lasers

Vertical cavity surface emitting lasers (VCSELs), take a different approach, where light propagates parallel to the growth direction, longitudinally confined by distributed Bragg reflector (DBR) mirrors, and most typically gain and thermally guided in the transverse direction. Unfortunately, the two planar mirrors limits the lateral device dimensions that remain in single transverse mode operation. Vertical external cavity surface emitting lasers (VECSELs) avoid this coupling by replacing one of the mirrors with a curved external reflector, having strong control modal control, while the gain is simply controlled by carrier injection. While electrically pumped VECSELs have been developed and commercially employed,[4] carrier diffusion ultimately limits electrically-pumped power scaling to mode sizes of 7.6×10^{-5} cm^2, limiting them to similar power scales as the SCOWL . Optically pumped VECSELs (also known as "optically pumped semiconductor lasers" - OPSLs), on the other hand, are not limited in this respect because the optical pump uniformity dictates the carrier population, making them strong candidates for achieving very high powers. Therefore, these lasers can scale to mode sizes on the order of 500 μm in diameter, and approach powers greater than 40 W[5,6] utilizing single chips. A schematic of a typical VECSEL cavity can be seen in Figure 1a.

There are several effects limiting power in this type of laser, dominated by thermal effects, causing the gain to fall out of resonance with the resonant periodic gain (RPG),[7] the subcavity resonance, as well as overall reduced gains. While laterally guided amplified spontaneous emission can limit the lateral mode size practical, it remains a secondary effect in power limitations, although practical VECSELs have modal gain diameters remaining lower than about 1 mm, commensurate with the lateral lasing threshold previously determined.[8]

Another method of power scaling is to increase the number of quantum wells in the longitudinal direction. Using multiple chips within a single cavity alleviates thermal power densities, that can reach many 10's of kW/cm^2. This was first introduced achieving about 20 W from two chips, each operating independently with about 11 W,[9] while maintaining an M^2 beam parameter of $\sim$2. More recently, Coherent has shown three chips scaled in a similar fashion, achieving a dramatic 50 W of frequency-doubled light,[10] while maintaining M^2 <1.3.

Finally, because they are based around semiconductor material, one may take advantage of the vast number of material systems to provide fundamental output between 650 nm and 2.8 μm,[5,11–17] based on the AlGaAs/GaAs or InGaAs/GaAs systems, the InGaAsP/InP, or the InGaSb/GaSb growth system, depending on the wavelength desired. This can be extended through intracavity nonlinear elements outside this region by non-linear up-conversion[18] and down-conversion.[19]

2. FABRICATION

The relatively simple VECSEL fabrication process adds another level of attractiveness to universities who may not have state-of-the-art fabrication facilities as well as commercial entities who are able to achieve higher yields as a result of the low-tolerance fabrication requirements. For the sake of high power, the most critical step is heat removal, and is often considered more as a "packaging" step rather than fabrication. The process generally follows one of two approaches, depending on the grown structure. Because the thermal densities produced can easily reach 10's of kW/cm^2, it becomes necessary to increase the area in which this thermal power is dissipated, thus reducing the heat density. Therefore, in almost all cases, a heat-spreader is utilized.

2.1 Surface-emitter

If the epitaxy is grown such that the DBR mirror is closest to the substrate, followed by an active region growth, we denote this as a "surface-emitter". Chips of desired size (typically <5 mm×5 mm) are cleaved from a wafer, perhaps after the substrate is thinned to ease singulation. In this case, it is rather inefficient to remove the heat through the DBR and the substrate, so either a compression bond or a capillary bond is made between the surface of the epitaxy and a transparent heat conductor such as SiC or transparent single crystal diamond. This bond must be as intimate as possible to promote heat conduction out of the surface of the semiconductor. The transparent heat conductor is then put in contact with a heat-sink which removes the heat laterally, still allowing an annular opening such that it does not interfere with the optical mode.

Unless AR coated, this intracavity heat-spreader acts as a flow-finesse Fabry-Pérot filter, and the longitudinal modes are filtered by its free-spectral range. For lower powers, the intracavity heat spreader is not essential. Indeed, most of the early VECSELs relied on heat conduction through a thinned substrate of less than 100 μm.

2.2 Substrate-emitter

When an etch-stop is first grown, followed by the active region is first epitaxially grown and a DBR structure, we refer to this as a "substrate emitter". In this case, fabrication is somewhat complicated, although it alleviates the the need for an intracavity heat-spreader which removes the heat laterally. First, the epitaxy is is metalized (before or after singulation) in conjunction with a heat-spreader, which does not need to be of optical quality. The two materials are soldered together using an appropriate solder. One must consider solder thermal conductivity, coefficient of thermal expansion (CTE) mismatch between the semiconductor and the heat-spreader, solder temperature, as well as total solder thickness, which should be kept to a minimum. The substrate and potentially etch-stop is then removed through chemical and/or mechanical means, taking it out of the optical cavity. In some cases, an anti-reflection coating is then put on the exposed surface of the semiconductor (as may be done in the surface-emitter as well). The heat-spreader is put in direct contact with a heat-sink.

In substrate-emitters, the active-region heat source is directly pumped on top of the heat-sink, no lateral heat flow is necessarily required and the heat sink is a uniform distance from the heat source (the thickness of the heat-spreader plus the thickness of the DBR). This has shown to perform quite well in the near-IR (on GaAs substrates), even though the heat must propagate through the low thermal conductivity of the DBR. This method has not been yet utilized in the GaSb material system, where not only the material has a lower thermal conductivity, but the longer wavelength necessitates a thicker DBR.

3. VECSEL SMALL AND LARGE SIGNAL DYNAMICS

For many applications relevant to sensing, including LADAR, chemical sensing, RF Photonics, free-space communications, the temporal laser response becomes vital to determining whether a laser is suitable for use. VECSELs have a rich history of passive mode-locking through incorporation of a semiconductor saturable absorber mirror (SESAM).[20,21] The simplicity of the cavity lends to potentially extremely short cavities with high repetition rates (c.f. Reference 21, where a folded cavity is demonstrated as short as 3 mm). Although, the short cavities allow for fast pulse repetitions, the semiconductor carrier lifetime tends to limit the peak pulse power.

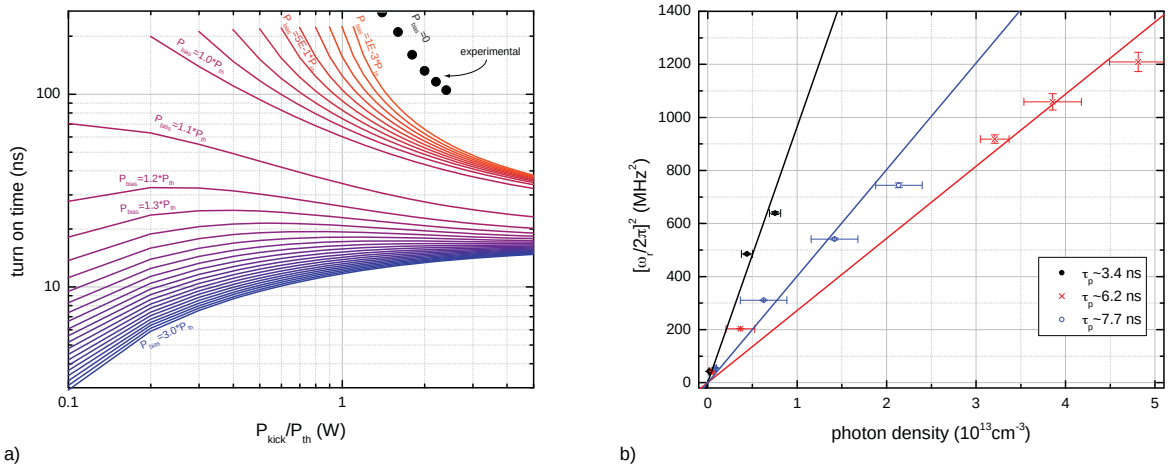

Figure 2. a) Solid lines represent computed turn-on times for a linear VECSEL with a photon lifetime of 3.45 ns, neglecting thermal effects. Each curve represents a bias pump power and a modulation "kick" such that the final pump power is $P_{bias} + P_{kick}$. The solid point data are experimental results from a pulsed VECSEL with similar photon lifetime. b) Experimental and fitted small-signal modulation representing bias pump powers above threshold. Each curve is a different photon lifetime.

The carrier lifetime, on the order of a few nanosceonds, and tends to be similar to photon lifetimes for typical cavities. The photon lifetime for a linear cavity is given by:

$$\frac{1}{\tau_p} = \frac{1}{2}\frac{cv_g}{v_g L_p + cL_a}\left[\ln\left(\frac{1}{R_1 R_2}\right) + \ln\left(\frac{1}{S^2}\right)\right], \tag{1}$$

where τ_p is the photon lifetime, c is the vacuum speed of light, v_g is the group velocity in the semiconductor material, L_p is the cavity length outside of the semiconductor, L_a is the length of the portion of the cavity inside the semiconductor*, $R_{1,2}$ are the mirror reflectivities, and S is the semiconductor surface scatter. When L_p is set to zero in Equation 1, this holds true for a standard VCSEL, however because L_a is on the order of microns, both mirror reflectivities are near unity, and the photon lifetime is only picoseconds. With most external cavity lasers, $L_p \gg L_a$ (i.e. $L_p \cong L_{tot}$), and therefore a good approximation for the photon lifetime is:

$$\frac{1}{\tau_p} \approx \frac{c}{2L_p}\left[\ln\left(\frac{1}{R_1 R_2}\right) + \ln\left(\frac{1}{S^2}\right)\right]. \tag{2}$$

One can see that for "typical" cavity lengths of a few millimeters to meters, this photon lifetime can span to regions both shorter and longer than the carrier lifetime. In fact, we may utilize this flexibility because unlike conventional semiconductor lasers, changes may be readily made to the cavity without significant effort.

One application for is using the laser ringing dynamics for high-sensitivity intracavity laser-absorption spectroscopy (ICLAS), used to identify trace gasses within the laser cavity.[22] These large-signal dynamics can be thought of as turn-on times of the VECSEL. When using spatially-averaged rate equations, such as those in Reference 23 for barrier pumped lasers, it is possible to numerically investigate how quickly one may turn on the laser (and subsequently turn-off the laser). When beginning from some bias-point (P_{bias}), where the laser is operating in steady-state, the pump may be suddenly changed to a new constant value ($P_{bias} + P_{kick}$). The laser reacts as a class-A or class-B laser, depending on the carrier and photon lifetimes. Figure 2a shows the

*Explicitly, then, the total cavity length is $L_{tot} = L_a + L_p$

time it takes to reach 98% of the final steady-state, which we will call the "turn on time", when the laser is nominally on the line between class-A and class-B. While this is a non-linear system which must be solved numerically, in the case of class-A laser, an approximate formula for lasers beginning from noise ($P_{bias} \ll P_{th}$) that effectively predicts the turn on time[24] may be used, and this is dominated by the initial to final state ratio and the photon lifetime, given in Equation 2. It should be noted in Figure 2a that the turn-on times as we have defined, are somewhat skewed, because the change in output power may remain within only a few percent of the final steady-state. This is especially true for low P_{kick}/P_{th} values. We show discrete date in Figure 2a for experimentally-obtained turn-on times for $P_{bias} = 0$, although the pump turn-on time itself finite, so there is an artificial offset associated with that time which is not accounted for in the experimental data.

To avoid thermal effects in semiconductor lasers, it is common to bias below threshold and pulse the laser for a short time. Some applications also require similar pulses. For example, infrared countermeasures require pulses on in the range of 0.5-50 ns.[25] It becomes clear that VECSELs must have a shorter lifetime than that shown in Figure 2a to achieve the full scale desired for such an application, and even then, biasing above threshold improves the speed rather significantly. For overcoming thermal effects, one should pulse well above the turn on time in order for the optical pulse to reach a quasi-cw state. Figure 2a shows a particular laser geometry where even at large values of P_{kick}, the turn on time asymptotically reaches about 25 ns. Pulses would therefore have to be nominally at least 10× this length to reasonably follow the pump. This turn-on delay can be seen in Figure 3 in Reference 26, and is studied in-depth in Reference 27.

An alternative to large signal modulation is small-signal modulation, commonly used for RF analog and digital signal, such as those used for optical communication. In this case, the response in a linear, shift-invariant filter in the RF domain to any signal imparted on it through modulating the pump. The modulation response function can be stated like the following:

$$H(\omega) \approx \frac{1}{1 + i\tau_{wb}\omega} \frac{\omega_r^2}{\omega_r^2 - \omega^2 + i\gamma\omega}. \tag{3}$$

The angular resonance frequency is ω_r, γ is the associated damping, and τ_{wb} is the barrier to well carrier lifetime,[28] which dominates over direct non-radiative recombination in the barriers. This function is completely analogous to electrically-injected semiconductor lasers through a step confinement heterostructure, where τ_{wb} is equivalent to the parasitic capacitance. Measured resonance frequencies are shown in Figure 2b as a function of laser power (within the cavity, scaled by volume).[23] Typical resonance frequencies are on the order of 20-50 MHz, while the 3-dB cut-off frequency is approximately the same because the damping is strong. There may be some ambiguity to the fitted data because we don't see all three poles possible in measured small-signal transfer functions that we would expect from Equation 3, though these numbers seem in line with others measured for shorter photon lifetime VECSEL cavities.[29] Because the carrier drift can be neglected in optically pumped structures, carriers excited in the barriers may take longer to decay into the wells than electrically injected lasers. This may make the τ_{wb} term significantly longer, causing an error in the fitting (where the strong damping would be due to the τ_{wb} term, rather than γ).

The large photon lifetime (on the order of nanoseconds) results in a direct small signal modulation that is impractical for high-speed communication, where GHz are typically expected. However, without a strong resonance, the random intensity noise (RIN) of the VECSEL also can result in a low additive phase noise for RF optical links.[29] The residual phase noise is mainly due to pump noise that is passed by Equation 3, a low-pass filter. Thus remote transmission and distribution of microwave local oscillators may be an appropriate application for VECSELs, without the need for complicated injection/feedback loops for linewidth stabilization.

4. SYSTEMS OF VECSELS

As stated previously, VECSELs provide an ideal platform for inclusion of nonlinear optical elements such as frequency-converting crystals and SESAMs. However, it is also possible to include other nonlinear elements, such as other VECSEL cavities. In principal, we may expand the laser cavity to a system of optical cavities and gain elements, which may naturally lead to new behavior. In the slow regime, we chose to ignore all terms

relative to N_b and arrive at a generalize I gain-element, J cavity set of coupled ordinary differential equations:

$$\frac{d}{dt}N_i = \frac{\Omega_w}{(\hbar\omega_p V_w)}P_i - \frac{N_i}{\tau_i} - v_g g_i \sum_j^J \frac{\Gamma_i^{(j)}}{\tilde{\Gamma}_i^{(j)}} S^{(j)} \quad (4)$$

$$\frac{d}{dt}S^{(j)} = -\frac{S^{(j)}}{\tau_p^{(j)}} + v_g S^{(j)} \sum_i^I \Gamma_i^{(j)} g_i \quad (5)$$

In these equations, N_i is the carrier density in chip i, and $S^{(j)}$ is the photon density in optical cavity j. $\Omega_w/(\hbar\omega_p V_w)$ is the number of carriers produced for a unit power, and we have assumed this is the same for all chips. The carrier lifetime of the i^{th} chip is given by τ_i, while the photon lifetime is $\tau_p^{(j)}$ for the j^{th} cavity in the system. The gain for each chip is g_i, the group velocity is v_g. The mode/gain overlap of cavity j with gain chip i is given by $\Gamma_i^{(j)}$. Finally, the ratio of overlaps in Equation 4 accounts for chips that may see multiple passes in a cavity as well as the contribution of each chip's RPG enhancement.

The simplest case, containing a single chip and two cavities is pictured schematically in Figure 3a. In this case, Equations 4 and 5 become:

$$\frac{d}{dt}N = \frac{\Omega_w}{(\hbar\omega_p V_w)}P - \frac{N}{\tau} - v_g g\left(\Gamma_{r1}S^{(1)} + 2\Gamma_{r2}S^{(2)}\right) \quad (6)$$

$$\frac{d}{dt}S^{(1)} = -\frac{S^{(1)}}{\tau_p^{(1)}} + v_g g\Gamma^{(1)}S^{(1)} + \beta^{(1)}BN^2 \quad (7)$$

$$\frac{d}{dt}S^{(2)} = -\frac{S^{(2)}}{\tau_p^{(2)}} + v_g g\Gamma^{(2)}S^{(2)} + \beta^{(2)}BN^2 \quad (8)$$

Spontaneous emission is explicitly returned to Equation 7 and 8, as it turns out they become critically important to what happens at the boundary. It is possible to include a birefringent filter into each cavity, and tune the cavity overlap of each cavity independently, over the boundary where $\Gamma^{(2)}\tau_p^{(2)} = \Gamma^{(1)}\tau_p^{(1)}$, where we can turn either of the lasers completely off. This boundary is unstable and not achievable in practice due to noises in real systems. However, in practice, we do see that both lasers can lase simultaneously.

When spontaneous emission is included, the gain coupling can prevent one cavity running away and the other shutting off completely. Consider the case shown in Figures 3b-d and 3c where cavity 1 and cavity 2 are very near the areas of equal threshold. Cavity 1 begins blocked and is unblocked at time $t = 0$. The uncoupled threshold of cavity 1 is initially slightly lower and the photon density increases at the expense of the photon density of cavity 2. As the photon density of cavity 2 drops, the relative contribution of the spontaneous emission increases. Because spontaneous emission is an additive term to the photon equation, it can be considered as a mechanism for reducing the threshold gain of cavity 2, thus lowering the uncoupled threshold of cavity 2 below that of cavity 1 and effectively reducing the photon density of cavity 1. This cycle is damped by the photon lifetime allowing both cavities to operate simultaneously. This effective reduction in the threshold is of course, very small, which is why this effect is important only when the two uncoupled thresholds are very close. When they are slightly farther away, one achieves the quickest switching effect, mitigated by the photon lifetimes of each cavity, as well as the carrier lifetime of the chip. This effect can be seen in Figure 3.

5. CONCLUSIONS

VECSELs have been improved over the last decade to the point where they have shown their utility for many high-brightness laser applications. The high-gain semiconductor, combined with the ability to effectively separate control of the gain relative to the mode size proves to be critical to creating lasers which have powers approaching 100 W of single spatial mode output. Inclusions of intracavity spectral selection allows active, non-thermal tuning allowing for spectrometry applications such as stand-off chemical analysis. Moreover, their flexibility and open architecture allows for changes on the fly, suiting them to varied types of systems.

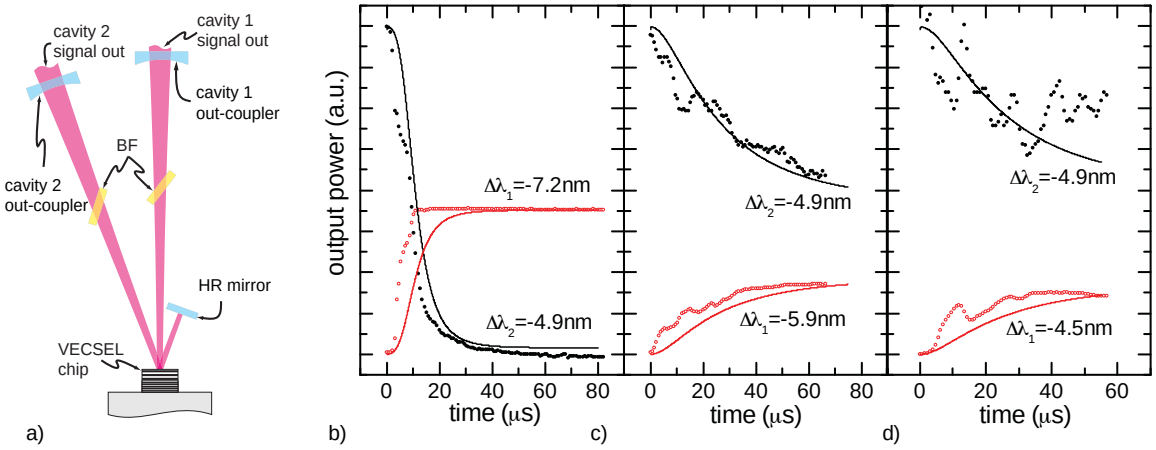

Figure 3. a) Schematic of a two-cavity VECSEL system centered around a single gain chip. b-d) Plots of output power versus time for different cavity tunings in a two cavity, one chip VECSEL system. Cavity 1 was chopped in the dual cavity configuration. b) Cavity tuned such that cavity switches from completely on to completely off c)-d) various tuning such that the switching is less complete. Simulated results are shown as solid lines.

Their dynamics, while not naturally fast, provide interesting capabilities, and potential for low noise oscillators. With access to cavity parameters such as length and out-coupler reflectivity, we can tune the photon lifetime using a single chip, thus potentially getting very different dynamical responses with a simple geometric change. Moreover it is relatively trivial to combine multiple chips or multiple cavities to obtain sometimes unpredictable responses.

ACKNOWLEDGMENTS

This work was supported by AFOSR through lab task 08RY08COR.

REFERENCES

1. O. Hess, S. Koch, and J. Moloney, "Filamentation and beam propagation in broad-area semiconductor lasers," *IEEE J. of Quant. Elect.* **31**, pp. 35 –43, Jan. 1995.
2. W. Both, G. Erbert, A. Klehr, R. Rimpler, G. Stadermann, and U. Zeimer, "Catastrophic optical damage in GaAlAs/GaAs laser diodes," *Optoelectronics, IEE Proceedings J* **134**, p. 95, Feb 1987.
3. R. Huang, J. Donnelly, L. Missaggia, C. Harris, J. Plant, D. Mull, and W. Goodhue, "High-power nearly diffraction-limited AlGaAs-InGaAs semiconductor slab-coupled optical waveguide laser," *IEEE Photon. Tech. Lett.* **15**, pp. 900 –902, Jul 2003.
4. J. McInerney, A. Mooradian, A. Lewis, A. Shchegrov, E. Strzelecka, D. Lee, J. Watson, M. Liebman, G. Carey, B. Cantos, W. Hitchens, and D. Heald, "High-power surface emitting scmiconductor laser with extended vertical compound cavity," *Elect. Lett.* **39**, pp. 523–525, Mar. 2003.
5. T.-L. Wang, Y. Kaneda, J. Yarborough, J. Hader, J. Moloney, A. Chernikov, S. Chatterjee, S. Koch, B. Kunert, and W. Stolz, "High-power optically pumped semiconductor laser at 1040 nm," *IEEE Photon. Tech. Lett.* **22**, pp. 661 –663, May 2010.
6. J. Moloney, "personal correspondence." jml@acms.arizona.edu.
7. S. Corzine, R. Geels, J. Scott, R. H. Yan, and L. Coldren, "Design of Fabry-Perot surface-emitting lasers with a periodic gain structure," *IEEE J. of Quant. Elect.* **25**(6), pp. 1513–1524, 1989.
8. R. Bedford, M. Kolesik, J. Chilla, M. Reed, T. Nelson, and J. Moloney, "Power-limiting mechanisms in VECSELs," in *Proc. SPIE - Int. Soc. Opt. Eng.*, **5814**, pp. 199–208, SPIE, 2005.

9. L. Fan, M. Fallahi, J. Hader, A. R. Zakharian, J. V. Moloney, J. T. Murray, R. Bedford, W. Stolz, and S. W. Koch, "Multichip vertical-external-cavity surface-emitting lasers: a coherent power scaling scheme," *Opt. Lett.* **31**, pp. 3612–3614, Dec 2006.
10. L. E. Hunziker, Q.-Z. Shu, D. Bauer, C. Ihli, G. J. Mahnke, M. Rebut, J. R. Chilla, A. L. Caprara, H. Zhou, E. S. Weiss, and M. K. Reed, "Power-scaling of optically pumped semiconductor lasers," *Solid State Lasers XVI: Technology and Devices* **6451**(1), p. 64510A, SPIE, 2007.
11. J. E. Hastie, S. Calvez, M. D. Dawson, T. Leinonen, A. Laakso, J. Lyytikäinen, and M. Pessa, "High power CW red VECSEL with linearly polarized TEM_{00} output beam," *Opt. Exp.* **13**, pp. 77–+, Jan. 2005.
12. L. Fan, C. Hessenius, M. Fallahi, J. Hader, H. Li, J. V. Moloney, W. Stolz, S. W. Koch, J. T. Murray, and R. Bedford, "Highly strained InGaAs/GaAs multiwatt vertical-external-cavity surface-emitting laser emitting around 1170 nm," *App. Phy. Lett.* **91**(13), p. 131114, 2007.
13. H. Lindberg, M. Strassner, J. Bengtsson, and A. Larsson, "Optically pumped vecsel operating at 1550 nm," *Proc. SPIE - Int. Soc. Opt. Eng.* **5364**, pp. 25 – 33, (San Jose, CA, United states), 2004.
14. A. Härkönen, M. Guina, O. Okhotnikov, K. Rößner, M. Hümmer, T. Lehnhardt, M. Müller, A. Forchel, and M. Fischer, "1-W antimonide-based vertical external cavity surface emitting laser operating at 2-μm," *Opt. Exp.* **14**, pp. 6479–6484, July 2006.
15. B. Rosener, N. Schulz, M. Rattunde, C. Manz, K. Kohler, and J. Wagner, "GaSb-based VECSEL exhibiting multiple-watt output power and high beam quality at a lasing wavelength of 2.25 μm," *Proc. SPIE - Int. Soc. Opt. Eng.* **6997**, pp. 699702 – 1, (USA), 2008.
16. N. Schulz, M. Rattunde, C. Ritzenthaler, B. Rosener, C. Manz, K. Kohler, J. Wagner, and U. Brauch, "Resonant optical in-well pumping of an (AlGaIn)(AsSb)-based vertical-external-cavity surface-emitting laser emitting at 2.35 μm," *App. Phy. Lett.* **91**(9), pp. 091113 – 1, 2007.
17. B. Rösener, M. Rattunde, R. Moser, S. Kaspar, C. Manz, K. Köhler, and J. Wagner, "GaSb-based optically pumped semiconductor disk lasers emitting in the 2.0-2.8 μm wavelength range," *Solid State Lasers XIX: Technology and Devices* **7578**(1), p. 75780X, SPIE, 2010.
18. L. Fan, T.-C. Hsu, M. Fallahi, J. Murray, R. Bedford, Y. Kaneda, J. Hader, A. Zakharian, J. Moloney, W. Stolz, and S. Koch, "Tunable watt-level blue-green vertical-external-cavity surface-emitting lasers by intracavity frequency doubling," *App. Phy. Lett.* **88**, pp. 251117–1 – 251117–3, June 2006.
19. D. J. Stothard, J.-M. Hopkins, D. Burns, and M. H. Dunn, "Stable, continuous-wave, intracavity, optical parametric oscillator pumped by a semiconductor disk laser (VECSEL)," *Opt. Exp.* **17**, p. 10648, Jun 2009.
20. R. Häring, R. Paschotta, A. Aschwanden, E. Gini, F. Morier-Genoud, and U. Keller, "High-power passively mode-locked semiconductor lasers," *IEEE J. of Quant. Elect.* **2**, pp. 1268–1275, Sept. 2002.
21. D. Lorenser, D. Maas, H. Unold, A.-R. Bellancourt, B. Rudin, E. Gini, D. Ebling, and U. Keller, "50-GHz passively mode-locked surface-emitting semiconductor laser with 100-mw average output power," *IEEE J. of Quant. Elect.* **42**(8), pp. 838 – 47, 2006.
22. A. Garnache, A. A. Kachanov, F. Stoeckel, and R. Houdré, "Diode-pumped broadband vertical-external-cavity surface-emitting semiconductor laser applied to high-sensitivity intracavity absorption spectroscopy," *J. of Opt. Sci. of Am. B* **17**, pp. 1589–1598, Sep 2000.
23. M. Walton, N. Terry, J. Hader, J. Moloney, and R. Bedford, "Extraction of semiconductor microchip differential gain by use of optically pumped semiconductor laser," *App. Phy. Lett.* **95**(11), p. 111101, 2009.
24. A. Siegman, *Lasers*, University Sciences Books, 1986.
25. H. Bekman, J. van den Heuvel, F. van Putten, and R. Schleijpen, "Development of a mid-infrared laser for study of infrared countermeasures techniques," *Proc. SPIE - Int. Soc. Opt. Eng.* **5615**(1), pp. 27 – 38, (USA), 2004.
26. J. M. Yarborough, Y.-Y. Lai, Y. Kaneda, J. Hader, J. V. Moloney, T. J. Rotter, G. Balakrishnan, C. Hains, D. Huffaker, S. W. Koch, and R. Bedford, "Record pulsed power demonstration of a 2 μm GaSb-based optically pumped semiconductor laser grown lattice-mismatched on an AlAs/GaAs Bragg mirror and substrate," *App. Phy. Lett.* **95**, pp. 081112 –081112–3, Aug 2009.
27. S. Chatterjee, W. Diehl, S. Horst, K. Hantke, W. W. Stolz, A. Thranhardt, S. W. Koch, P. Brick, M. Furitsch, S. Illek, I. Pietzonka, J. Luft, and W. W. Ruhle, "Nanosecond to microsecond dynamics of 1040 nm semiconductor disk lasers," in *Technical Digest Series, QELS 2007*, p. 4431387, IEEE, 2007.

28. L. Coldren and S. Corzine, *Diode Lasers and Photonic Integrated Circuits*, John Wiley & Sons, Inc., 1995.
29. G. Baili, M. Alouini, T. Malherbe, D. Dolfi, J.-P. Huignard, T. Merlet, J. Chazelas, I. Sagnes, and F. Bretenaker, "Evidence of ultra low microwave additive phase noise for an optical rf link based on a class-a semiconductor laser," *Opt. Exp.* **16**(14), pp. 10091–10097, 2008.